Visnyk NTUU KPI Seriia – Radiotekhnika Radioaparatobuduvannia, 2025, Iss. 99, pp. 5–14

UDC 621.396.6

Development and Research of Three-Channel Power Divider for the Decimeter Range

Fabirovskyy S. Ye., Storozh V. H., Prudyus I. N., Matiieshyn Yu. M., Sidelnyk I. V.

Lviv Polytechnic National University, Lviv, Ukraine

E-mail: *fabirovskii@gmail.com*

The work is devoted to the development and research of a three-channel decimeter range power divider. Power dividers are widely used in all branches of radio electronics and wireless communication systems, in particular in radio communication systems, radio monitoring systems and others. At the first stage of research, a three-channel divider was calculated based on the Wilkinson scheme, implemented on quarter-wave line sections. To minimize losses in the divider, air-filled coaxial line sections were used for its implementation. The ballast resistance system is implemented according to the triangle scheme, which made it possible to minimize its parasitic inductance. The expansion of the operating frequency band is achieved by using a two-stage scheme with an additional quarter-wave line section. At the second stage of the research, the parameters of the developed divider were simulated in the Micro-Cap 12 program, which is currently freely available. For this purpose, the serial parameters of all line sections of the divider were calculated. The simulation showed that in the range from 350 MHz to 550 MHz, the isolation between the channels is no worse than -23.2 dB, and at the central frequency – no worse than -40 dB. At the third stage, a research of the implemented experimental prototype of the three-channel divider was carried out. As the research showed, the transmission coefficient from the input to any of the output channels of the divider in the entire operating frequency band is no worse than -4.8 dB, and the reflection coefficient from the input is no worse than -20 dB, which indicates its high efficiency. The isolation between the channels at the boundary of the operating range is no worse than -22 dB and is heading to -40 dB in its central part. The results of the experimental research coincide well with the modeling results in the Micro-Cap 12 program, which confirms the reliability of the numerical calculation and the correct choice of the divider model.

Keywords: power divider; electromagnetic waves; S-parameters; decimeter range; radio frequency devices

DOI: 10.20535/RADAP.2025.99.5-14

Introduction

In the field of high-frequency technology and wireless communications, there is a continuously growing demand for efficient and reliable power dividing devices. The development and research of such devices are highly relevant, as they play an important role in ensuring signal quality indicators and optimizing energy characteristics in information transmission systems.

Wilkinson Power Dividers are widely used in modern wireless communication systems and in the construction of antenna arrays for radio engineering systems [1–3]. They enable the distribution of the power from a signal source among consumers while ensuring a high level of isolation between them.

There are numerous implementations of power dividers, both using distributed parameter elements and lumped parameter elements. Power dividers based on reactive lumped elements have better mass and dimensional characteristics but a narrower operational bandwidth [4]. This limitation does not apply to dividers using lumped resistive elements [5], but they are characterized by higher signal splitting losses and weak isolation between output channels. Currently, significant attention is devoted to the development and research of power dividers based on microstrip lines, including symmetric designs [6, 7], devices based on these structures offer high technological efficiency and parameter repeatability.

In particular, [8] presents the development and research results of a broadband microstrip three-channel power divider. While achieving a bandwidth of more than 200 percent, the study does not address the degree of uniformity among the output channels in terms of transmission coefficient and mutual isolation.

The work in [9] proposes an effective implementation of a three-channel power divider using specific apertures in the ground structure of the microstrip line on which it is based (Defected Ground Structure – DGS). The paper provides experimental research results. However, it is worth noting that in microstrip-based dividers, signal losses can reach significant values [10, 11]. Evidently, in complex circuit implementations

and cascaded divider configurations, these losses will accumulate.

Therefore, the purpose of this work is to develop and research a three-channel power divider based on coaxial lines with an air-filled dielectric, ensuring minimal signal power losses and a high level of isolation between output channels. The research was conducted in the decimeter wavelength range. The research aims to create an efficient device that ensures uniform power distribution among three channels while maintaining high efficiency and operational stability.

The study examines and research the key aspects of construction and using power dividers in microwave technology. It outlines the methodology for calculating the structural parameters of the divider, considering the need to widen the bandwidth, and analyzes the impact of these parameters on the characteristics of three-channel power divider. Additionally, the choice of the type of feeder line for optimal device implementation is justified.

The results of the electrical parameter of the divider modeling and experimental studies of the implemented prototype confirmed the correctness of the theoretical assumptions. This work opens new prospects for creating highly efficient and reliable power dividers that can be used in modern communication systems and wireless technologies.

1 Implementation of a three-channel power divider

Dividers and combiners are electronic devices used for dividing or combining radio frequency (RF) signals. They are essential components in RF systems and technologies, where efficient management and processing of RF signals are required. In an ideal power divider (Fig. 1,a) the power entering port 3 is evenly distributed between the two output ports, 1 and 2. Conversely, in a power combiner (Fig. 1, b) the power of the signals from input ports 1 and 2 is combined at the output port 3 [12].

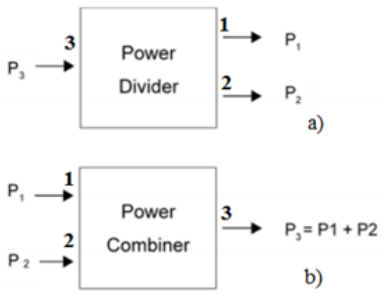

Fig. 1. Power divider a); and power combiner b)

The precise functioning of dividers (combiners) depends on their design and characteristics. These devices can be implemented using passive components (resistors, capacitors and inductors) or active components (transistors). They can be utilized in a wide range of applications, including mobile communication, radio monitoring, radar systems, satellite technology, and many others.

One of the earliest and most well-known power dividers is the Wilkinson divider (Fig. 2). Ernest Wilkinson first published this design in 1960, and it continues to be widely used in RF communication systems.

The Wilkinson power divider is implemented using quarter-wavelength sections of feeder lines, ensuring matching regime across all its ports and providing good isolation between the output ports, which is largely determined by a ballast resistor with a value of $2W$, where W is the characteristic impedance of the main line.

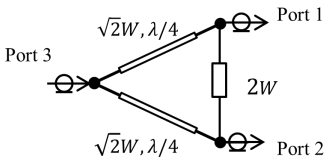

Fig. 2. Wilkinson power divider

There are other types of power dividers, such as resistive power dividers. However, they have low isolation between ports and significant signal losses (Fig. 3).

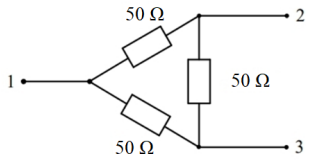

Fig. 3. Resistive power divider

A power divider with a division factor of 2^n, where n is an integer, can be easily implemented using a cascaded connection of identical two-way dividers. The entire structure can be realized in a planar form, such as on a printed circuit board. However, when power needs to be divided into an odd number of parts, a transition to a volumetric design is required, which complicates the implementation of the ballast resistor scheme.

In such power dividers (combiners), two methods are used for implementing the ballast resistor scheme: the “star” configuration and the “triangle” configuration. For example, in Fig. 4 a three-channel Wilkinson divider in the “star” configuration is shown. The impedance of the branches is $\sqrt{3}W$, while the impedance of the resistors is W [13].

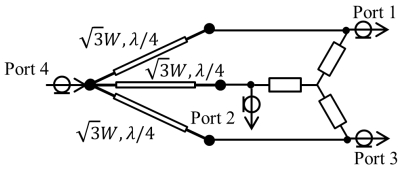

Fig. 4. Three-channel Wilkinson divider in the "star" configuration

The following figure shows a three-channel Wilkinson power divider in the "triangle" configuration. Its branches again have an impedance of $\sqrt{3}W$, but the resistors now have an impedance of $3W$.

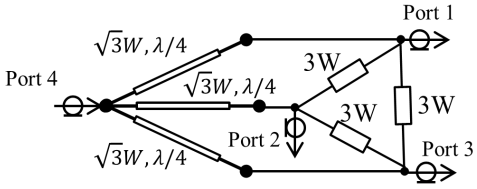

Fig. 5. Three-channel Wilkinson divider in the "triangle" configuration

In both cases, the design of the divider is volumetric. However, the "triangle" configuration allows for minimizing the impact of the parasitic parameters of the ballast resistors on the general indicators of the device.

2 Calculation of the characteristic impedances of the divider's line segments

In the studied frequency range from 350 MHz to 550 MHz, the center frequency is 450 MHz. Therefore, the wavelength in free space is equal to

$$\lambda_0 = \frac{c}{f} = \frac{300}{450} \approx 0.667\,\text{m}. \tag{1}$$

The quarter-wavelength is approximately 167 mm, which determines the lengths of the divider's line segments and will be refined during the course of the study.

Let us determine the number of cascades in the divider. We will calculate the characteristic impedances of the divider's segments. From the generator side, the internal impedance is equal to the characteristic impedance, i. e., $W = 50\ \Omega$. From the load side, we have three identical resistances, each of which is also equal to the characteristic impedance $R_L = W = 50\ \Omega$. Since the generator power must be evenly distributed among these loads, this is equivalent to having these resistances connected in parallel. Therefore, their total impedance is

$$R_\Sigma = \left(\frac{1}{W}+\frac{1}{W}+\frac{1}{W}\right)^{-1} = \left(3\cdot\frac{1}{50}\right)^{-1} \approx 16.7\,\Omega. \tag{2}$$

As a result, the system will be inconsistent.

Therefore, before connecting the loads $R_L = 50\ \Omega$, their impedances must be transformed to $R = 150\ \Omega$ using quarter-wavelength transformers W_T. After this transformation, their parallel connection will provide the required impedance of 50 Ω, as shown in Fig. 6.

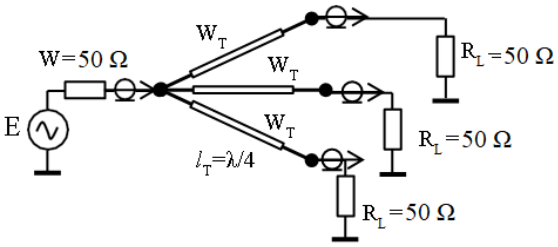

Fig. 6. Division of a microwave signal using quarter-wavelength line segments

The characteristic impedance of a transformer is determined using the expression

$$W_T = \sqrt{W\cdot R} = \sqrt{50\cdot 150} \approx 86.6\,\Omega. \tag{3}$$

The frequency analysis of this circuit, taking into account the influence of the quarter-wavelength segments on the device's bandwidth, is performed based on expression (4).

$$Z = W_T \cdot \frac{R_L + jW_T\cdot \text{tg}\left(\frac{2\pi f}{V\phi}l_T\right)}{W_T + jR_L\cdot \text{tg}\left(\frac{2\pi f}{V\phi}l_T\right)}, \tag{4}$$

where Z is the input impedance of a segment of the feeder line with a length l_T and a characteristic impedance W_T, loaded with an impedance R_L, which, in general, may be complex and frequency-dependent;

$V\phi$ is the phase velocity in the line used for the quarter-wavelength transformer. For a line with air as the dielectric, the phase velocity v equals the speed of light c;

f is the frequency at which the calculation is performed. This expression will be repeatedly used for frequency analysis.

As a result, three such impedances are connected in parallel to the signal source. Since all impedances are identical, the total impedance, analogous to expression (2), will be three times smaller:

$$Z_\Sigma = \frac{Z}{3}. \tag{5}$$

The reflection coefficient, which for comparison will be expressed directly in decibels, is calculated using the equation

$$S11 = 20\cdot \lg\left(\left|\frac{Z_\Sigma - W}{Z_\Sigma + W}\right|\right). \tag{6}$$

The frequency analysis is shown in Fig. 7. As seen from the graph, the frequency bandwidth at a reflection coefficient level of –20 dB is 100 MHz, which corresponds to 22 percent. This is insufficient for operation within the specified frequency range.

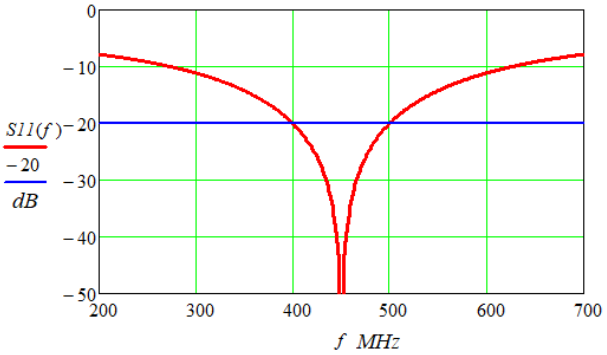

Fig. 7. Frequency analysis of a single-stage three-channel divider

To widen the bandwidth, it is proposed to implement a two-stage three-channel power divider. In this case, the characteristic impedances of the line segments are calculated analogously to the calculation of a two-stage quarter-wavelength transformer [14] for matching the impedances R_Σ and W.

The characteristic impedance of the first arm is

$$W_{T1} = \sqrt{W \cdot \sqrt{W \cdot R_\Sigma}} = \sqrt{50 \cdot \sqrt{50 \cdot 16.7}} \approx 38\,\Omega. \quad (7)$$

The characteristic impedance of the second arm is

$$W_{T2} = \sqrt{R_\Sigma \cdot \sqrt{W \cdot R_\Sigma}} = \sqrt{16.7 \cdot \sqrt{50 \cdot 16.7}} \approx 22\,\Omega. \quad (8)$$

The value of the characteristic impedance of the second arm is an auxiliary parameter. Using it, we determine how the impedance of the main line $W = 50\ \Omega$ is transformed through the segment W_{T1} into the section between W_{T1} and W_{T2}:

$$R_{12} = \frac{W_{T1}^2}{W} = \frac{38^2}{50} \approx 28.9\,\Omega. \quad (9)$$

The impedance transformation in the two-stage quarter-wavelength transformer is shown in Fig. 8.

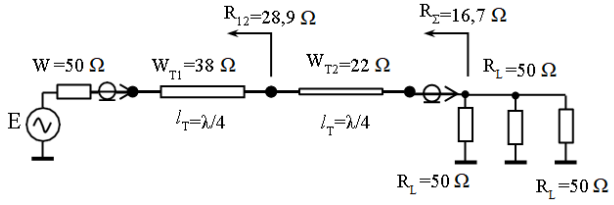

Fig. 8. Impedance transformation in the two-stage quarter-wavelength transformer

Therefore, the resulting load impedance of the three arms of the divider, transformed by the cascade with the characteristic impedance W_{T2}, should be 28.9 Ω so, the impedance of each arm should be three times greater than the value of R_{12}:

$$R_n = 3 \cdot R_{12} = 3 \cdot 28.9 \approx 86.7\,\Omega. \quad (10)$$

Thus, the quarter-wavelength segment of each arm line should transform the impedance $R_L = 50\ \Omega$ not to 150 Ω, as in the single-stage divider, but to 86,7 Ω. We calculate its characteristic impedance as for a standard quarter-wavelength transformer

$$W_{T3} = \sqrt{R_n \cdot W} = \sqrt{86.7 \cdot 50} \approx 65.8\,\Omega. \quad (11)$$

As a result, the three segments with characteristic impedances W_{T3} transform the load impedances of 50 Ω for each channel into an impedance of 86,7 Ω. These impedances are then added in parallel, resulting in a total impedance of 28,9 Ω. In the final stage, this impedance is transformed by the segment W_{T1} with a characteristic impedance of 38 Ω into 50 Ω, which corresponds to the impedance of the feeder line. A schematic representation of such a divider is shown in Fig. 9, and the frequency analysis based on the described algorithm is presented in Fig. 10.

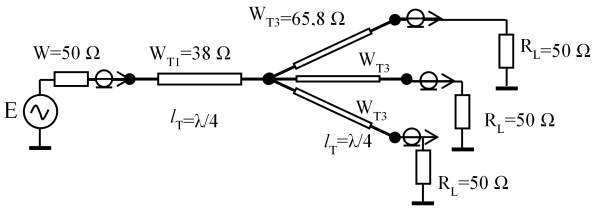

Fig. 9. A schematic representation of a two-stage three-channel power divider

As seen from the frequency analysis, the reflection coefficient does not exceed -20 dB in the working frequency band from 324 MHz to 576 MHz, which covers the specified range. The bandwidth is 252 MHz, or 56 percent.

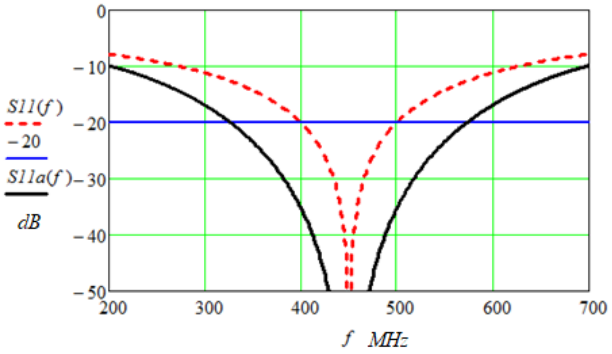

Fig. 10. Frequency analysis of a two-stage three-channel power divider

Thus, by introducing an additional quarter-wavelength segment of the feeder line, the working frequency bandwidth has been expanded by a factor of 2.5 compared to the single-stage divider, with only a slight increase in the complexity of the design. For

comparison, the frequency characteristic of the single-stage three-channel power divider is shown in Fig. 10 by the dashed line.

3 Justification for the choice of feeder line type for the implementation of the power divider

The complete circuit of the three-channel power divider is shown in Fig. 11. As mentioned in the first chapter, power dividers can be implemented using different types of feeder lines.

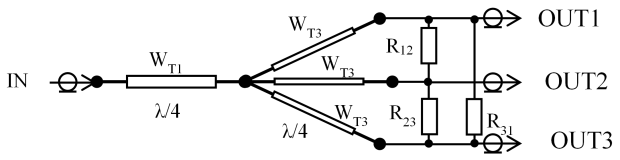

Fig. 11. The circuit of the three-channel power divider

From a constructive perspective, it is more convenient to implement power dividers with a number of channels that is a multiple of two. In this case, by sequentially cascading division by two, a planar design can be achieved in strip line configuration. However, in our case, for the implementation of a three-channel power divider, the use of coaxial lines and the construction of a volumetric design will be more appropriate.

This is due to, firstly, the relatively low frequency range from 350 MHz to 550 MHz, which also implies the bulkiness of the printed circuit board, secondly, in a strip line configuration, it is impossible to ensure channel splitting identity. A power divider additionally requires the presence of so-called ballast resistors, with a nominal value that is n times (n – the number of channels) greater than the nominal characteristic impedance of the main line [15]. The ballast resistors $R12$, $R23$, and $R31$ are placed between the outputs of the divider. For our case, the number of channels $n = 3$, and the characteristic impedance of the main line is 50 Ω. Therefore, the nominal values of the ballast resistors are $3 \cdot 50 = 150$ Ω.

3.1 Analysis of the requirements for the manufacturing accuracy of the feeder line segments of the divider

When selecting the type of connector for the power divider implementation, preference was given to N-Type connector. Unlike SMA connectors, N-Type connectors are characterized by significantly higher mechanical reliability and can operate at higher power levels. For the implementation of the experimental prototype, the NC-305-T coaxial connector was chosen.

The body of this connector is well-matched with a standard copper tube with an inner diameter of 13 mm and a wall thickness of 1 mm, making it convenient for the implementation of the experimental prototype. In this case, it will be convenient to use a feeder line with air dielectric. Therefore, in the subsequent calculations, it is assumed that the inner diameter of the outer conductor of the coaxial lines, on which the elements of the power divider will be implemented, is 13 mm.

It is known [16], that the characteristic impedance of a coaxial line can be determined using the formula

$$W = \frac{60}{\sqrt{\varepsilon}} \cdot \ln\left(\frac{D}{d}\right), \tag{12}$$

where ε is relative permittivity, in our case $\varepsilon = 1$; D – the inner diameter of the outer conductor, in our case, is 13 mm; d – the outer diameter of the inner conductor.

Using the given formula, taking into account that $\varepsilon = 1$, we will calculate the diameters of the inner conductors for the lines $W_{T1} = 38$ Ω and $W_{T3} = 65,8$ Ω. The diameter of the inner conductor for the lines with a characteristic impedance of $W_{T1} = 38$ Ω is

$$d_1 = \exp\left(-\frac{W_{T1}}{60}\right) \cdot D = \exp\left(-\frac{38}{60}\right) \cdot 13 = 6.9\,\text{mm}. \tag{13}$$

The diameter of the inner conductor for the lines with a characteristic impedance $W_{T3} = 65,8$ Ω is

$$d_3 = \exp\left(-\frac{W_{T3}}{60}\right) \cdot D = \exp\left(-\frac{65.8}{60}\right) \cdot 13 = 4.3\,\text{mm}. \tag{14}$$

To evaluate the influence of dimensions on the characteristic impedance, we will plot the dependence of the characteristic impedance on the diameter of the inner conductor using expression (12). The graph (Fig. 12) highlights the diameters of the inner conductors that ensure the required characteristic impedances. At the same time, it is evident that the slope of the graph is not constant. This indicates that the absolute error in manufacturing the inner conductors will affect the percentage deviation of the characteristic impedance from its nominal value differently.

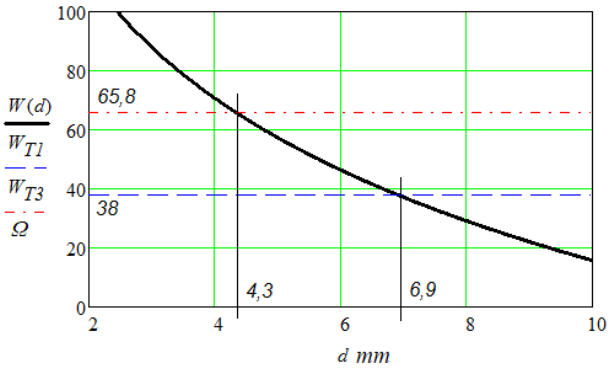

Fig. 12. The dependence of the characteristic impedance of a coaxial line on the diameter of the inner conductor at $D = 13$ mm

To analyze the magnitude of this influence, we take the derivative of expression (12) and present this dependence in Fig 13. Thus, this dependence reflects the sensitivity of the characteristic impedance to changes in the diameter of the inner conductor.

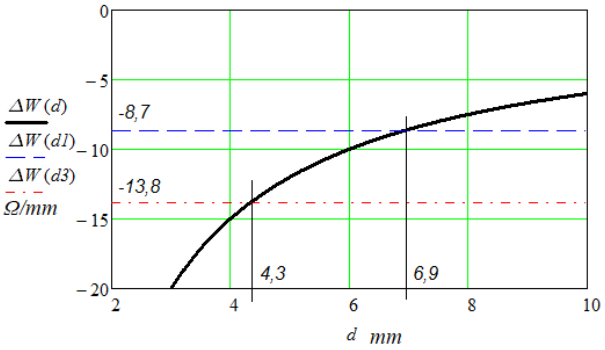

Fig. 13. The dependence of the sensitivity of the characteristic impedance to changes in the diameter of the inner conductor at $D = 13$ mm

To stay within the established limits of ±5 percent deviation from the nominal characteristic impedance for the section with characteristic impedance $W_{T1} = 38\ \Omega$, the diameter of the inner conductor should be manufactured with an accuracy of no worse than $\pm 0,22$ mm, and for sections with characteristic impedance $W_{T3} = 65,8\ \Omega$ – $\pm 0,23$ mm. It can be considered that the absolute accuracy of the inner conductor diameters implementation is practically the same. In practical realization, it is sufficient for this to be $\pm 0,2$ mm.

4 The electrical parameters of a power divider modeling

4.1 Calculation of the parameters of the equivalent power divider circuit

To carry out the modeling, it is necessary to determine the serial parameters of the feeder line segments of the divider. Specifically, these are the serial capacitance and the serial inductance.

The known system of equations that relates the serial parameters of the feeder line to its characteristic impedance and phase velocity is as follows:

$$\begin{cases} W = \sqrt{\frac{L}{C}} \\ V\phi = \frac{1}{\sqrt{LC}} \end{cases}, \qquad (15)$$

where W – the characteristic impedance of the given feeder line, Ω; $V\phi$ – the phase velocity in the line, m/s; L – the serial inductance, H/m; C – the serial capacitance, F/m.

In our case, the line is air-filled, so $V\phi = c = 3 * 10^8$ m/s. Thus, given the specified characteristic impedance and phase velocity, from the system of equations (15), the serial parameters for the first stage of the divider, with a characteristic impedance of $W_{T1} = 38\ \Omega$, the serial inductance is

$$L_{T1} = \frac{W_{T1}}{V\phi} = \frac{38}{3 \cdot 10^8} \approx 127\,\text{nH}, \qquad (16)$$

the serial capacitance is

$$C_{T1} = \frac{1}{W_{T1} \cdot V\phi} = \frac{1}{3 \cdot 10^8 \cdot 38} \approx 88\,\text{pF}. \qquad (17)$$

For the line segments of the second stage of the divider, with a characteristic impedance $W_{T3} = 65,8\ \Omega$, the serial inductance is

$$L_{T3} = \frac{W_{T3}}{V\phi} = \frac{65.8}{3 \cdot 10^8} \approx 219\,\text{nH}, \qquad (18)$$

the serial capacitance is

$$C_{T3} = \frac{1}{W_{T3} \cdot V\phi} = \frac{1}{3 \cdot 10^8 \cdot 65.8} \approx 51\,\text{pF}. \qquad (19)$$

It is also necessary to determine the equivalent circuit of the ballast resistor, as it is known that at high frequencies, the inductive component of the resistor's impedance becomes significant. For the prototype implementation, metal oxide resistors with wire leads and a power rating of 1 W were selected.

It was experimentally determined that within the specified frequency range, the resistors used have an active resistance component of $R = 149,7\ \Omega$, and an inductive reactance component of $XL = +10,7\ \Omega$ at a frequency of $f = 450$ MHz, corresponding to an inductance of

$$L = \frac{X_L}{2\pi f} = \frac{10.7}{2\pi 450 \cdot 10^6} \approx 3.8\,\text{nH}. \qquad (20)$$

Thus, during modeling, the ballast resistors should be represented by a series equivalent circuit consisting of an ideal resistor with a nominal value of 149,7 Ω and an ideal inductor with a nominal value of 3,8 nH. The presence of the inductive component will necessitate some adjustments to the second-stage divider segments, which will be determined during the modeling process. Consequently, all parameters required for the simulation are prepared. This allows for conducting the study using the Micro-Cap 12 software, which is freely available and effective for simulating electronic circuits, particularly those involving equivalent circuit models.

4.2 Modeling and analysis of results

As a result, the equivalent circuit of the power divider in the Micro-Cap 12 program is presented in Fig. 14.

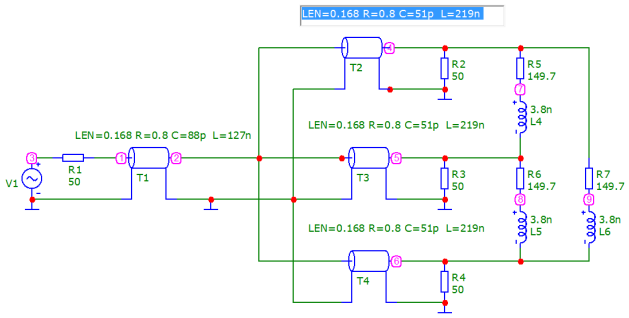

Fig. 14. Power divider equivalent circuit in the Micro-Cap 12 program

In Fig. 14 $V1$ – the signal source with an internal resistance of 50 Ω, accounted for by the introduction of resistor $R1 = 50$ Ω. $T1$ – is a segment of the feeder line of the first stage of the power divider with a characteristic impedance of $W_{T1} = 38$ Ω. For the operation of the program, the line length is set as LEN = 0,168 m, its serial resistance as $R = 0,8$ Ω/m, as well as the serial capacitance $C = C_{T1} = 88$ pF and serial inductance $L = L_{T1} = 127$ nH.

$T2$, $T3$, and $T4$ are segments of the feeder lines of the second stage of the power divider with a characteristic impedance of $W_{T3} = 65,8$ Ω. An example of the $T2$ segment shows the window for entering the primary parameter values. Their nominal values are visible in the figure.

The elements $R2 = R3 = R4 = 50$ Ω are the load resistances corresponding to the first, second, and third channels, respectively.

The elements $R5L4$, $R6L5$ and $R7L6$ are ballast resistors, taking into account the parasitic inductance.

During the research, the power distribution of the signal source $V1$ among the channels was determined, as well as the isolation between the divider channels. The simulation results in the program are presented in Fig. 15.

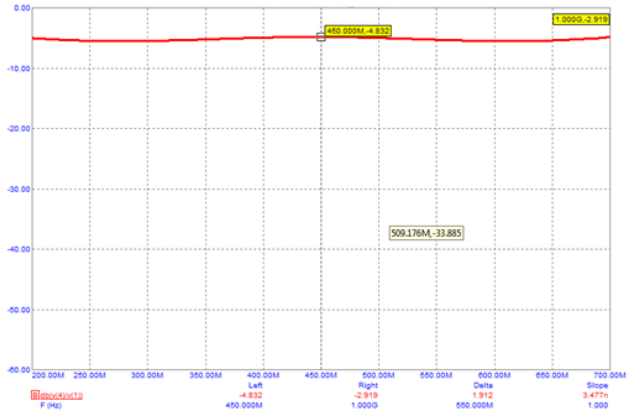

Fig. 15. Research of the frequency dependence of the splitting coefficient

The theoretical value of the splitting coefficient for the three-channel divider, without considering losses, is -4,77 dB. According to the simulation results, at the center frequency, the value is -4,83 dB with a slight decrease at the edges of the bandwidth.

This difference is primarily caused by the presence of losses in real lines. In the experimental prototype, there will also be additional losses at the transitions between the divider lines and the RF connectors, which will lead to a further decrease in the divider's transmission coefficient.

Next, the study of the isolation between the channels is conducted. Isolation between the divider channels is a necessary condition for its operation when the loads are different or during a fault condition in one of the channels. In this case, the presence of ballast resistors ensures the normal operation of the functional channels.

The circuit for conducting the isolation research between channels is shown in Fig. 16.

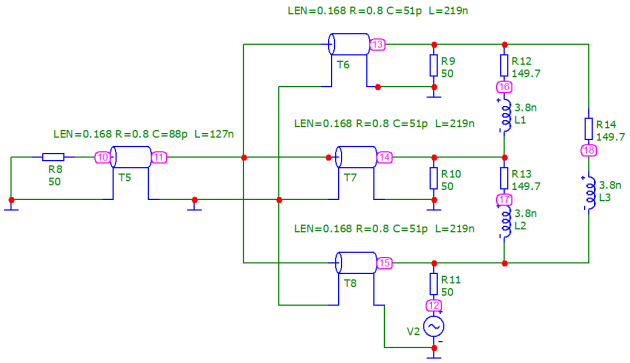

Fig. 16. Research of the isolation between the divider channels

In this case, the signal source $V2$ with an internal resistance $R11 = 50$ Ω, which equals the characteristic impedance, is connected to the third channel. The signal level is then measured at the load resistance $R10 = 50$ Ω of the second channel. The simulation result is shown in Fig. 17. As seen from the simulation results, the isolation between the channels is below -20 dB across a sufficiently wide frequency range.

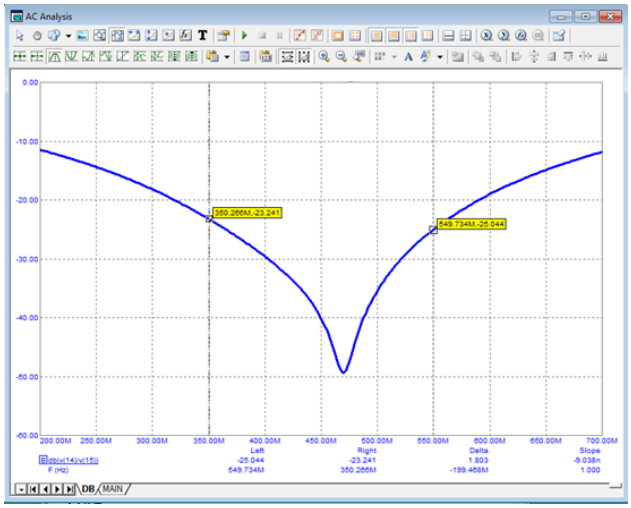

Fig. 17. Research of the isolation between the divider channels

At the lower frequency of the range, 350 MHz, the isolation is -23.2 dB, meaning less than 0.5 percent of the input power at the third channel's input leaks into the loads of the other channels. At the upper frequency of the range, 550 MHz, the isolation is -25.0 dB, meaning approximately 0.3 percent of the input power at the third channel's input leaks into the loads of the other channels. At the central frequency, the isolation is -40 dB, meaning only 0.01 percent of the input power at the third channel's input leaks into the loads of the other channels.

5 Implementation of the prototype of power divider experimental model

As a result of the conducted analysis and calculations, a coaxial line with air dielectric was selected, the characteristic impedances of the quarter-wavelength line segments of the divider were determined, and their lengths were calculated.

The quarter-wavelength line segment of the first stage has a characteristic impedance of $W_{T1} = 38$ Ω. With an inner conductor diameter of 13 mm, determined by the selected coaxial connector type NC-305-T, the inner conductor diameter is 6.9 mm. The three quarter-wavelength line segments of the second stage have characteristic impedances of $W_{T3} = 65,8$ Ω. With the inner diameter of the screen of this line 13 mm, the inner conductor diameter is 4.3 mm. The length is 168 mm.

The prototype of power divider experimental model is presented in Fig. 18. The output connectors of the divider are marked with numbers 1, 2, and 3, while the input connector is marked with number 4.

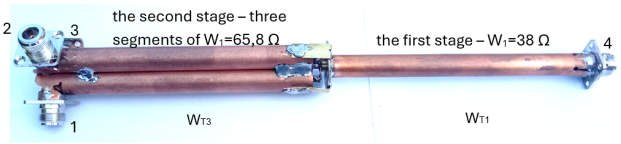

Fig. 18. The prototype of power divider experimental model

The characteristic impedance of the first stage of the divider is 38 Ω. The three feeder line segments of the second stage of the divider arranged in parallel, have a characteristic impedance of 65.8 Ω.

As mentioned earlier, ballast resistors are used in dividers to ensure isolation between channels. In this case, three ballast resistors with a nominal value of 150 Ω have been used. The resistors are connected in a "triangle" configuration, which minimizes the parasitic inductance of the connections (Fig. 19).

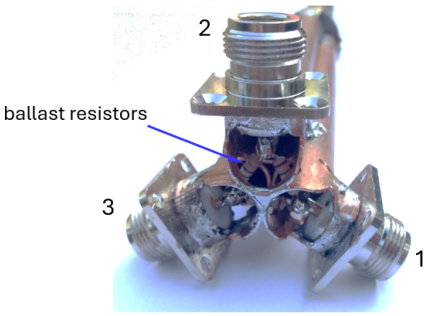

Fig. 19. Ballast resistors between the output connectors of the divider

The prototype uses metal-oxide resistors with wire leads. Their parameters in the operating range were determined earlier. Unlike other types of resistors, they are sufficiently reliable and exhibit a weak dependence of resistance on frequency, which is especially important when operating at high and very high frequencies. During assembly, the wire leads of the resistors were shortened.

6 Description of the experimental setup and research of power divider parameters

The measuring setup consists of a personal computer, the NANOVNA-V2 computer extension, and the object under study – the power divider. The vector analyzer provides measurements in the range from 50 kHz to 3 GHz for key parameters such as reflection coefficient (S11), transmission coefficient (S21), standing wave ratio (SWR), and complex impedance (Re(Z) and Im(Z)). The measured data is displayed on the PC, with the capability to store the measurement results in the form of electronic spreadsheets.

The measuring setup for the experimental research of the power divider parameters is shown in Fig. 20.

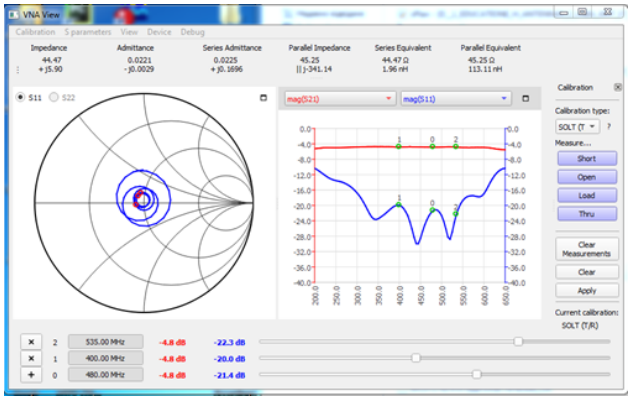

Fig. 20. Measuring setup for the experimental research of the power divider parameters

Figure 21 shows the measurement results of the transmission coefficient mag(S21) from the output of the divider and the reflection coefficient from its input mag(S11). In this case, the signal was transmitted from the input of the divider (connector 4) to one of its outputs (connector 1).

The figure shows both measured values in a logarithmic scale. From the graph, it is evident that the transmission coefficient mag(S21) remains almost constant across the entire frequency range, not dropping below -4.8 dB. This means that, compared to the ideal case (-4.77 dB), the losses is only 0.03 dB. Meanwhile, the reflection coefficient mag(S11) is less than -20 dB. This indicates that the divider is well matched with the feeder line, with more than 99 percent of the power being delivered to the load. The results obtained from the outputs of the other channels (connectors 2 and 3) are identical and therefore are not presented here.

In the next experiment, the isolation between channels was investigated. In this case, the signal was applied from connector 3 to connector 2. The results of the investigation are shown in Fig. 21.

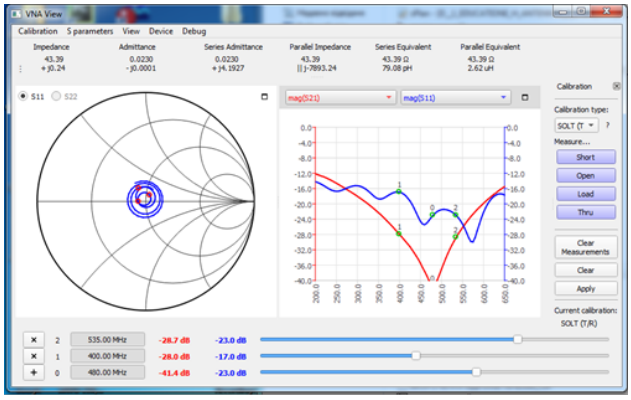

Fig. 21. The results of the isolation between channels measurement, mag(S21), and the reflection coefficient, mag(S11)

As seen from the experimental results, the isolation between channels (mag(S21)) is no worse than -24 dB. This means that, in the operating frequency range, in the worst case, only approximately 0.4 percent of the power can leak from one channel to another, which is a good result.

At the same time, the reflection coefficient (mag(S11)) at the central frequency is -24 dB, which is an excellent result. In the worst case, at a frequency of 400 MHz, some deterioration to -17 dB occurs, but this is not critical, as the device continues to operate in a matched condition. Only 2 percent of the power is lost due to reflection.

Conclusions

The research and development of a three-channel power divider for the decimeter range is a relevant and perspective task in the context of modern high-frequency technologies. The obtained results and conclusions can be summarized as follows.

During the analysis of power dividers in microwave technology, their purpose, design principles, requirements, and applications within high-frequency technologies were identified. The methodology for analyzing electrical parameters and the component base for implementing such devices were thoroughly examined.

The development of the three-channel power divider involved calculating the characteristic impedances of line segments, studying the influence of cascade characteristic impedances on device characteristics, and justifying the choice of the feeder line type. An analysis of the manufacturing precision requirements for feeder line segments provided the necessary technical foundations for implementation of the divider.

Experimental research confirmed the efficiency of the developed three-channel power divider. Electrical parameter modeling and analysis of the results provided the basis for implementation of a prototype of the experimental sample. The conducted experimental studies validated the correctness of the chosen implementation principles.

Thus, the research results indicate the successful completion of the outlined tasks. High potential of the developed three-channel power divider for use in modern high-frequency data transmission systems and wireless technologies has been confirmed by modeling results and experimental studies.

References

[1] Huang, T.-Y. and Lee, Y.-J. (2024). Design of Microstrip Antenna Arrays with Rotated Elements Using Wilkinson Power Dividers for 5G Customer Premise Equipment Applications. *International Journal of Antennas and Propagation*, 2945195, 15 p. DOI: 10.1155/2024/2945195.

[2] Richa, Sharma, M. M., Jha, C. G., Yadav, S., Garg, J. and Sharma, I. (2021). Design and Performance Evaluation of Wilkinson Power Divider. *2021 IEEE Indian Conference on Antennas and Propagation (InCAP)*, pp. 31-33. DOI: 10.1109/InCAP52216.2021.9726188.

[3] Saleh, S., Ismail, W., Zainal Abidin, I. S., Jamaluddin, M. H., Bataineh, M. H., & Alzoubi, A. S. (2020). N-way compact ultra-wide band equal and unequal split tapered transmission lines wilkinson power divider. *Jordanian Journal of Computers and Information Technology*, Vol. 6, Iss. 3, pp. 291-302. doi: 10.5455/jjcit.71-1590536342.

[4] Jamshidi, M. B., Roshani, S., Talla, J. et al. (2021). Size reduction and performance improvement of a microstrip Wilkinson power divider using a hybrid design technique. *Scientific Reports*, Vol. 11, Article number: 7773. DOI: 10.1038/s41598-021-87477-4.

[5] Pant, P., Shrivastava, N., Arora, M. and Paliwal, R. (2023). Wilkinson Power Divider. *International Journal for Research in Applied Science and Engineering Technology*, Vol. 11, Iss. 1, pp. 163-169. DOI: 10.22214/ijraset.2023.51432.

[6] Razzaz, F., Saeed, S. M. and Alkanhal, M. A. S. (2022). Compact Ultra-Wideband Wilkinson Power Dividers Using Linearly Tapered Transmission Lines. *Electronics*, Vol. 11, Iss. 19, 3080. DOI: 10.3390/electronics11193080.

[7] Go, D.-J., Min, B.-C., Kim, M.-J., Choi, H.-C. and Kim, K.-W. (2024). Compact Ultra-Wideband Wilkinson Power Divider in Parallel Stripline with Modified Isolation Branches. *Sensors*, Vol. 24, Iss. 11, 3437. DOI: 10.3390/s24113437.

[8] Patankar, S. and Suhel, M. (2020). Design and Analysis of 3-Way Power Divider for UWB Applications. *International Research Journal of Engineering and Technology (IRJET)*, Vol. 7, Iss. 11, pp. 250-252.

[9] Chhit, S., Lee, J. B., Ahn, D. and Jang Y. (2024). Wide-Bandwidth Wilkinson Power Divider for Three-Way Output Ports Integrated with Defected Ground Structure. *Journal of information and communication convergence engineering*, Vol. 22, Iss. 1, pp. 14-22. DOI: 10.56977/jicce.2024.22.1.14.

[10] Chaitanya, D. M. K., Ch, D., Reddy, T. V. and Jarupula, S. (2020). Two Way Equal Power Divider. *International Research Journal of Engineering and Technology (IRJET)*, Vol. 7, Iss. 5, pp. 5109-5114.

[11] Duru, İ. (2022). Design and Simulation of Equal Split Wilkinson Power Divider. *Avrupa Bilim Ve Teknoloji Dergisi*, Iss. 39, pp. 59-62. DOI: 10.31590/ejosat.1148431.

[12] Keysight Technologies, 2016-2021, Published in USA, March 10, 2021, 5992-1632EN 3.

[13] Three-Way Planar Wilkinsons. *Microwaves101*, date of access: 7 December 2024.

[14] Ouf, E. G., El-Hassan, M. A., Farahat, A. E., Hussein, K. F. A. and Mohassieb, S. A. (2022). Wideband Impedance Matching Balun for Balanced Two-Arm Antennas Fed with Coaxial Line. *2022 International Telecommunications Conference (ITC-Egypt)*, pp. 1-8. DOI: 10.1109/ITC-Egypt55520.2022.9855689.

[15] Grebennikov, A. (2008). Power Combiners, Impedance Transformers and Directional Couplers: Part II. *High Frequency Electronics*, pp. 42-53.

[16] Off-Center Coax. *Microwaves101*, date of access: 8 December 2024.

Розроблення та дослідження триканального подільника потужності дециметрового діапазону

Фабіровський С. Є., Сторож В. Г., Прудиус І. Н., Матієшин Ю. М., Сідельник І. В.

Робота присвячена розробленню та дослідженню триканального подільника потужності дециметрового діапазону. На першому етапі дослідження було проведено розрахунок триканального подільника на базі схеми Вілкінсона, який реалізовано на чвертьхвильових відрізках ліній. Для мінімізації втрат у подільнику для його реалізації використані відрізки коаксіальних ліній з повітряним заповненням. Система баластних опорів реалізована за схемою трикутник, що дозволило мінімізувати її паразитну індуктивність. Розширення робочої смуги частот досягнуто застосуванням двокаскадної схеми з додатковим чвертьхвильовим відрізком лінії. На другому етапі дослідження здійснено моделювання параметрів розробленого подільника в програмі Micro-Cap 12, яка на даний час є у вільному доступі. Для цього були розраховані первинні (погонні) параметри усіх відрізків ліній подільника. Моделювання показало, що в діапазоні від 350 МГц до 550 МГц розв'язка між каналами не гірше -23,2 дБ, а на центральній частоті – не гірше -40 дБ. На третьому етапі здійснено дослідження реалізованого експериментального зразка триканального подільника. Як показали дослідження, коефіцієнт передавання з входу на будь-який з вихідних каналів подільника у всій робочій смузі частот не гірше -4,8 дБ, а коефіцієнт відбиття від входу не гірше -20 дБ, що свідчить про його високу ефективність. Ізоляція між каналами на межі робочого діапазону не гірше -22 дБ, і прямує до -40 дБ в його центральній частині. Результати експериментальних досліджень добре співпадають з результатам моделювання в програмі Micro-Cap 12, що підтверджує достовірність числового розрахунку і правильний вибір моделі подільника.

Ключові слова: подільник потужності; електромагнітні хвилі; S-параметри; дециметровий діапазон; радіочастотні пристрої